We confirmed that the same numbers of cells were applied to the kit by counting cell numbers.

In situ PLA

We used the Duolink (Olink, Uppsala, Sweden) kit for *in situ* PLA assay as previously described [40]. Combination of the primary antibodies was determined so that each antibody does not cross-react with the PLA probe-conjugated secondary antibody to the other primary antibodies. TOTO-3 (Invitrogen-Molecular Probes) or Vectashield mounting medium with DAPI (Vector laboratories) was used as a nuclear counterstain.

Promoter-reporter and cDNA constructs

Human PAI-1 reporter and 9× CAGA reporter were previously described [18]. Human Smad3, Smad4 and TTF-1 cDNAs were prepared as previously reported [25, 28]. Adenoviral expression vectors of LacZ and TTF-1 were prepared as described [28].

Dual-luciferase assay

Cells in 24-well plates were transfected with combinations of promoter-reporter constructs and expression plasmids using Lipofectamine LTX (Life Technologies). Total amounts of transfected DNA were adjusted to the same quantities with empty vectors. For normalization, pGL4.75-SV40-hRluc was cotransfected. Twenty-four hours later, cells were stimulated with or without 1 ng/ml TGF-β, and then harvested and assayed for luciferase activity 12 h after stimulation using the Dual-Luciferase Reporter Assay System (Promega). All samples were run in duplicate, and the results were averaged.

RNA interference

We used the siRNA against human TTF-1 (Invitrogen) as previously reported [28], and control siRNA was purchased from Invitrogen (Cat. 12935-112, sequence not available). siRNAs were introduced into A549 cells twice every 48 h using Lipofectamine RNAiMAX reagent (Invitrogen) according to the manufacturer's instructions. The final concentration of siRNA in the culture media was 50 nM.

Chromatin immunoprecipitation

A549 cells were cultured in 15-cm plates to ~80% confluence, and one plate was used for one immunoprecipitation. H441 cells were cultured in 10-cm plates, and two plates were used for one immunoprecipitation. ChIP was performed as described [21]. Re-ChIP assay was performed with a similar protocol, but the primary immune complex was eluted by 10 mM DTT at 37 °C for 30 min, diluted 50-fold with the ChIP-dilution Buffer as described [21] and immunoprecipitated with secondary antibodies. Fold-enrichment values were calculated by dividing percent input values at target regions by those at the first intron of *HPRT1* gene. Primer sequences for ChIP-qPCR are shown in Supplementary information, Data S1.

RNA isolation and qRT-PCR

Total RNAs were extracted as described previously [28]. First-strand cDNAs were synthesized using PrimeScript2 reverse transcriptase (TakaraBio, Shiga, Japan). qRT-PCR analysis was performed using FastStart Universal SYBR Green Master Mix with ROX (Roche), and the ABI PRISM 7000 Sequence Detection System or the StepONE Plus real time PCR system (Applied Biosystems, CA, USA). All samples were run in triplicate and the results were averaged. Primer sequences for qRT-PCR are shown in Supplementary information, Data S1.

ChIP-seq and data analysis

High-throughput sequencing of the ChIP fragments was performed using the Illumina Genome Analyzer (Illumina) following the manufacturer's protocols. One flow cell lane was used to sequence each pooled sample. Unfiltered 36-bp sequence reads were aligned against the human reference genome (NCBI Build 36, hg18) using ELAND (Illumina). Peaks were called using CisGenome v1.2 [41] by two-sample analysis; input genomic DNA was used as a negative control. Assigning a binding site to the nearest gene within 100 kb of a peak was performed using CisGenome. CisGenome was also used for both *de novo* motif prediction and motif mapping of TTF-1 ChIP-seq-binding regions.

Expression microarray

Total RNAs were extracted as described above. The experimental procedures for GeneChip (Affymetrix) were performed as described previously [21] using the GeneChip Human U133 plus 2.0 oligonucleotide arrays (Affymetrix). Microarray Suite software 5.0 (Affymetrix) was used with a target intensity of 100. Data from one array were obtained for each sample. Functional Annotation Clustering function of DAVID 6.7 was used to identify top-enriched clusters by gene ontology analyses.

3C assay

We used Taqman Chromosome Conformation Kits (Life Technologies) for the 3C assay. H441 cells were cultured in 10-cm plates, and one plate was used for each 3C assay. *Eco*RI was used for digestion. qRT-PCR analysis was performed using Taqman gene expression master mix, and a LightCycler 480 (Roche, Switzerland) was used. All samples were run in quintuplicate and the results were averaged. Amplification data were quantified using the $\Delta\Delta C_t$ method (comparative threshold cycle method) and normalized using the human internal control attached to the kit. The sequences of the Taqman probe and primers for 3C assays are shown in Supplementary information, Data S1.

Statistical analysis

Student's *t*-test was used for two-sample analyses. Bonferroni test of the R program (http://www.r-project.org/) was used for multiple comparisons of the data.

Accession number

Raw sequencing data with peak calling results and microarray data are available at GEO (GSE51510).

Acknowledgments

We are grateful to Kaori Shiina, Hiroko Meguro and Keiko Yuki for technical assistance, as well as to members of the Miyazono laboratory for discussion and advice. This research was supported by KAKENHI (grants-in-aid for scientific research) on Innovative Area (Integrative Research on Cancer Microenvironment Network, 22112002 to KM) from the Ministry of Education, Culture, Sports, Science and Technology of Japan (MEXT), and

Scientific Research (S), 20221009 to HA and Research Activity Start-up, 24890039 to KI from MEXT. This research was also supported by the Ministry of Health, Labor, and Welfare of Japan (a grant to DK), and the Genome Network Project from MEXT (a grant to HA). DK is supported by a grant from Mochida Memorial Foundation for Medical and Pharmaceutical Research and Project for Development of Innovative Research on Cancer Therapeutics from MEXT. The authors declare no competing interests.

References

1 Boggaram V. Thyroid transcription factor-1 (TTF-1/Nkx2.1/TITF1) gene regulation in the lung. *Clin Sci (Lond)* 2009; **116**:27-35.
2 Zamecnik J, Kodet R. Value of thyroid transcription factor-1 and surfactant apoprotein A in the differential diagnosis of pulmonary carcinomas: a study of 109 cases. *Virchows Arch* 2002; **440**:353-361.
3 Moldvay J, Jackel M, Bogos K, *et al.* The role of TTF-1 in differentiating primary and metastatic lung adenocarcinomas. *Pathol Oncol Res* 2004; **10**:85-88.
4 Saad RS, Liu YL, Han H, Landreneau RJ, Silverman JF. Prognostic significance of thyroid transcription factor-1 expression in both early-stage conventional adenocarcinoma and bronchioloalveolar carcinoma of the lung. *Hum Pathol* 2004; **35**:3-7.
5 Anagnostou VK, Syrigos KN, Bepler G, Homer RJ, Rimm DL. Thyroid transcription factor 1 is an independent prognostic factor for patients with stage I lung adenocarcinoma. *J Clin Oncol* 2009; **27**:271-278.
6 Perner S, Wagner PL, Soltermann A, *et al.* TTF1 expression in non-small cell lung carcinoma: association with TTF1 gene amplification and improved survival. *J Pathol* 2009; **217**:65-72.
7 Winslow MM, Dayton TL, Verhaak RG, *et al.* Suppression of lung adenocarcinoma progression by Nkx2-1. *Nature* 2011; **473**:101-104.
8 Hosono Y, Yamaguchi T, Mizutani E, *et al.* MYBPH, a transcriptional target of TTF-1, inhibits ROCK1, and reduces cell motility and metastasis. *EMBO J* 2012; **31**:481-493.
9 Weir BA, Woo MS, Getz G, *et al.* Characterizing the cancer genome in lung adenocarcinoma. *Nature* 2007; **450**:893-898.
10 Kwei KA, Kim YH, Girard L, *et al.* Genomic profiling identifies TITF1 as a lineage-specific oncogene amplified in lung cancer. *Oncogene* 2008; **27**:3635-3640.
11 Kendall J, Liu Q, Bakleh A, *et al.* Oncogenic cooperation and coamplification of developmental transcription factor genes in lung cancer. *Proc Natl Acad Sci USA* 2007; **104**:16663-16668.
12 Tanaka H, Yanagisawa K, Shinjo K, *et al.* Lineage-specific dependency of lung adenocarcinomas on the lung development regulator TTF-1. *Cancer Res* 2007; **67**:6007-6011.
13 Yamaguchi T, Yanagisawa K, Sugiyama R, *et al.* NKX2-1/TITF1/TTF-1-induced ROR1 is required to sustain EGFR survival signaling in lung adenocarcinoma. *Cancer Cell* 2012; **21**:348-361.
14 Watanabe H, Francis JM, Woo MS, *et al.* Integrated cistromic and expression analysis of amplified NKX2-1 in lung adenocarcinoma identifies LMO3 as a functional transcriptional target. *Genes Dev* 2013; **27**:197-210.
15 Massague J. TGFbeta in cancer. *Cell* 2008; **134**:215-230.
16 Feng XH, Derynck R. Specificity and versatility in TGF-beta signaling through Smads. *Annu Rev Cell Dev Biol* 2005; **21**:659-693.
17 Yagi K, Goto D, Hamamoto T, Takenoshita S, Kato M, Miyazono K. Alternatively spliced variant of Smad2 lacking exon 3. Comparison with wild-type Smad2 and Smad3. *J Biol Chem* 1999; **274**:703-709.
18 Dennler S, Itoh S, Vivien D, ten Dijke P, Huet S, Gauthier JM. Direct binding of Smad3 and Smad4 to critical TGF beta-inducible elements in the promoter of human plasminogen activator inhibitor-type 1 gene. *EMBO J* 1998; **17**:3091-3100.
19 Mullen AC, Orlando DA, Newman JJ, *et al.* Master transcription factors determine cell-type-specific responses to TGF-beta signaling. *Cell* 2011; **147**:565-576.
20 Morikawa M, Koinuma D, Miyazono K, Heldin CH. Genome-wide mechanisms of Smad binding. *Oncogene* 2012; **32**:1609-1615.
21 Mizutani A, Koinuma D, Tsutsumi S, *et al.* Cell type-specific target selection by combinatorial binding of Smad2/3 proteins and hepatocyte nuclear factor 4alpha in HepG2 cells. *J Biol Chem* 2011; **286**:29848-29860.
22 Zhang Y, Handley D, Kaplan T, *et al.* High throughput determination of TGFbeta1/SMAD3 targets in A549 lung epithelial cells. *PLoS One* 2011; **6**:e20319.
23 Kim SW, Yoon SJ, Chuong E, *et al.* Chromatin and transcriptional signatures for Nodal signaling during endoderm formation in hESCs. *Dev Biol* 2011; **357**:492-504.
24 Brown S, Teo A, Pauklin S, *et al.* Activin/Nodal signaling controls divergent transcriptional networks in human embryonic stem cells and in endoderm progenitors. *Stem Cells* 2011; **29**:1176-1185.
25 Koinuma D, Tsutsumi S, Kamimura N, *et al.* Chromatin immunoprecipitation on microarray analysis of Smad2/3 binding sites reveals roles of ETS1 and TFAP2A in transforming growth factor beta signaling. *Mol Cell Biol* 2009; **29**:172-186.
26 Li C, Zhu NL, Tan RC, Ballard PL, Derynck R, Minoo P. Transforming growth factor-beta inhibits pulmonary surfactant protein B gene transcription through SMAD3 interactions with NKX2.1 and HNF-3 transcription factors. *J Biol Chem* 2002; **277**:38399-38408.
27 Minoo P, Hu L, Zhu N, *et al.* SMAD3 prevents binding of NKX2.1 and FOXA1 to the SpB promoter through its MH1 and MH2 domains. *Nucleic Acids Res* 2008; **36**:179-188.
28 Saito RA, Watabe T, Horiguchi K, *et al.* Thyroid transcription factor-1 inhibits transforming growth factor-beta-mediated epithelial-to-mesenchymal transition in lung adenocarcinoma cells. *Cancer Res* 2009; **69**:2783-2791.
29 Tagne JB, Gupta S, Gower AC, *et al.* Genome-wide analyses of Nkx2-1 binding to transcriptional target genes uncover novel regulatory patterns conserved in lung development and tumors. *PLoS One* 2012; **7**:e29907.
30 Dennis G Jr, Sherman BT, Hosack DA, *et al.* DAVID: Database for Annotation, Visualization, and Integrated Discovery. *Genome Biol* 2003; **4**:P3.
31 Levy L, Hill CS. Smad4 dependency defines two classes of transforming growth factor-beta (TGF-beta) target genes and distinguishes TGF-beta-induced epithelial-mesenchymal transition from its antiproliferative and migratory responses. *Mol*

Cell Biol 2005; **25**:8108-8125.
32 Ijichi H, Otsuka M, Tateishi K, *et al.* Smad4-independent regulation of p21/WAF1 by transforming growth factor-beta. *Oncogene* 2004; **23**:1043-1051.
33 He W, Dorn DC, Erdjument-Bromage H, Tempst P, Moore MA, Massague J. Hematopoiesis controlled by distinct TIF-1gamma and Smad4 branches of the TGFbeta pathway. *Cell* 2006; **125**:929-941.
34 Zhao X, Nicholls JM, Chen YG. Severe acute respiratory syndrome-associated coronavirus nucleocapsid protein interacts with Smad3 and modulates transforming growth factor-beta signaling. *J Biol Chem* 2008; **283**:3272-3280.
35 Yamaguchi T, Hosono Y, Yanagisawa K, Takahashi T. NKX2-1/TTF-1: An enigmatic oncogene that functions as a double-edged sword for cancer cell survival and progression. *Cancer Cell* 2013; **23**:718-723.
36 Maschler S, Wirl G, Spring H, *et al.* Tumor cell invasiveness correlates with changes in integrin expression and localization. *Oncogene* 2005; **24**:2032-2041.
37 Taylor MA, Amin JD, Kirschmann DA, Schiemann WP. Lysyl oxidase contributes to mechanotransduction-mediated regulation of transforming growth factor-beta signaling in breast cancer cells. *Neoplasia* 2011; **13**:406-418.
38 Niu DF, Kondo T, Nakazawa T, *et al.* Transcription factor Runx2 is a regulator of epithelial-mesenchymal transition and invasion in thyroid carcinomas. *Lab Invest* 2012; **92**:1181-1190.
39 Koinuma D, Shinozaki M, Nagano Y, *et al.* RB1CC1 protein positively regulates transforming growth factor-beta signaling through the modulation of Arkadia E3 ubiquitin ligase activity. *J Biol Chem* 2011; **286**:32502-32512.
40 Yamazaki T, Yoshimatsu Y, Morishita Y, Miyazono K, Watabe T. COUP-TFII regulates the functions of Prox1 in lymphatic endothelial cells through direct interaction. *Genes Cells* 2009; **14**:425-434.
41 Ji H, Jiang H, Ma W, Johnson DS, Myers RM, Wong WH. An integrated software system for analyzing ChIP-chip and ChIP-seq data. *Nat Biotechnol* 2008; **26**:1293-1300.

(**Supplementary information** is linked to the online version of the paper on the *Cell Research* website.)

Cancer Science
Japanese Cancer Association JCA
Open Access

Transforming growth factor-β-induced lncRNA-Smad7 inhibits apoptosis of mouse breast cancer JygMC(A) cells

Mayu Arase,[1] Kana Horiguchi,[1,4] Shogo Ehata,[1] Masato Morikawa,[2] Shuichi Tsutsumi,[3] Hiroyuki Aburatani,[3] Kohei Miyazono[1,2] and Daizo Koinuma[1]

[1]Department of Molecular Pathology, Graduate School of Medicine, The University of Tokyo, Tokyo, Japan; [2]Science for Life Laboratory, Ludwig Institute for Cancer Research, Uppsala University, Uppsala, Sweden; [3]Genome Science Division, Research Center for Advanced Science and Technology, The University of Tokyo, Tokyo

Key words

Apoptosis, breast cancer, long non-coding RNA, Smad7, transforming growth factor-β

Correspondence

Kohei Miyazono, Department of Molecular Pathology, Graduate School of Medicine, The University of Tokyo, 7-3-1 Hongo, Bunkyo-ku, Tokyo 113-0033, Japan.
Tel: +81-3-5841-3345; Fax: +81-3-5841-3354;
E-mail: miyazono@m.u-tokyo.ac.jp

[4]Present address: Research Division, Discovery Pharmacology Department 2, Chugai Pharmaceutical Co. Ltd., 200 Kajiwara, Kamakura, Kanagawa, 247-8530, Japan.

Funding Information

Ministry of Education, Culture, Sports, Science and Technology of Japan (MEXT); Ministry of Health, Labor, and Welfare of Japan; Swedish Cancer Foundation; Mochida Memorial Foundation for Medical and Pharmaceutical Research; Ishidsu Shun Memorial Scholarship; Japan Society for the Promotion of Science; Kanae Foundation for Research Abroad; ITO Genboku and SAGARA Chian Memorial Scholarship

Received February 19, 2014; Revised May 12, 2014; Accepted May 15, 2014

Cancer Sci (2014)

doi: 10.1111/cas.12454

Transforming growth factor (TGF)-β exhibits both pro-apoptotic and anti-apoptotic effects on epithelial cells in a context-dependent manner. The anti-apoptotic function of TGF-β is mediated by several downstream regulatory mechanisms, and has been implicated in the tumor-progressive phenotype of breast cancer cells. We conducted RNA sequencing of mouse mammary gland epithelial (NMuMG) cells and identified a long non-coding RNA, termed lncRNA-Smad7, which has anti-apoptotic functions, as a target of TGF-β. lncRNA-Smad7 was located adjacent to the mouse *Smad7* gene, and its expression was induced by TGF-β in all of the mouse mammary gland epithelial cell lines and breast cancer cell lines that we evaluated. Suppression of lncRNA-Smad7 expression cancelled the anti-apoptotic function of TGF-β. In contrast, forced expression of lncRNA-Smad7 rescued apoptosis induced by a TGF-β type I receptor kinase inhibitor in the mouse breast cancer cell line JygMC(A). The anti-apoptotic effect of lncRNA-Smad7 appeared to occur independently of the transcriptional regulation by TGF-β of anti-apoptotic DEC1 and pro-apoptotic Bim proteins. Small interfering RNA for lncRNA-Smad7 did not alter the process of TGF-β-induced epithelial–mesenchymal transition, phosphorylation of Smad2 or expression of the *Smad7* gene, suggesting that the contribution of this lncRNA to TGF-β functions may be restricted to apoptosis. Our findings suggest a complex mechanism for regulating the anti-apoptotic and tumor-progressive aspects of TGF-β signaling.

Cancer cells make use of the tumor-promoting aspects of certain cytokines, while inhibiting their tumor-suppressive functions. Inhibition of the apoptotic program is one of the strategies used by cancer cells to continue dysregulated proliferation and tumor formation. The anti-apoptotic Bcl-2 family proteins are often upregulated, while several pro-apoptotic BH3-only proteins are inhibited, either transcriptionally or functionally, through interference with the upstream signaling pathways.[1]

Transforming growth factor (TGF)-β family proteins are representative proteins that possess bidirectional roles during tumor progression.[2] TGF-β exhibits cytostatic effects on various epithelial cells; many cancer cells are refractory to the cytostatic signals induced by TGF-β. Instead, they undergo an epithelial–mesenchymal transition (EMT) in response to TGF-β through induction of several factors, leading to stimulation of tumor migration and invasion.[3] TGF-β also displays both pro-apoptotic and anti-apoptotic effects on epithelial cells in a context-dependent manner. We previously showed that endogenous TGF-β produced by cancer cells plays a protective role in starvation-induced apoptosis of mouse breast cancer JygMC(A) and 4T1 cells through induction of the basic helix-loop-helix protein DEC1 and suppression of the BH3-only protein Bim.[4,5] TGF-β also suppresses rapamycin-induced apoptosis of serum-starved human basal-type breast cancer cells (MDA-MB-231 cell line).[6]

High throughput analyses have revealed that only approximately one-quarter of the transcripts are protein coding and that there are many non-coding RNA (ncRNA) in mice.[7] ncRNA are categorized based on their size and function, and long non-coding RNA (lncRNA) form a family of long transcripts with more than 200 nucleotides.[8] A limited number of lncRNA have been found to have essential biological functions,[9–11] and little is known about whether the majority of lncRNA play a role in cancer cells; this is in contrast to the wealth of information currently available about the roles of microRNA (miRNA) family transcripts in cancer.[12]

In the present study, we identified a lncRNA, designated lncRNA-Smad7 during a search for TGF-β-regulated transcripts in mouse mammary gland epithelial cells (NMuMG cell line). Interestingly, we found that lncRNA-Smad7 exhibited an anti-apoptotic effect upon stimulation by TGF-β in the mouse breast cancer cell line JygMC(A).

Materials and Methods

Cell culture. The mouse breast cancer cell lines JygMC(A) and 4T1 were cultured in DMEM containing 10% FBS, 50 units/mL penicillin and 50 μg/mL streptomycin. The mouse mammary epithelial cell line NMuMG was cultured in the above medium supplemented with 10 μg/mL insulin. Cells were grown in a 5% CO_2 atmosphere at 37°C.

Reagents and antibodies. Recombinant TGF-β (TGF-β3) and the TGF-β type I receptor inhibitor SB431542 were purchased from R&D systems (Ixonia, WI, USA) and Sigma-Aldrich (St. Louis, MO, USA), respectively. The following antibodies were used: rabbit anti-phospho-Smad2 (Cell Signaling Technology, Danvers, MA, USA.), mouse anti-α-tubulin (DM1A [Sigma-Aldrich]), mouse anti-Smad2/3 (BD Biosciences,

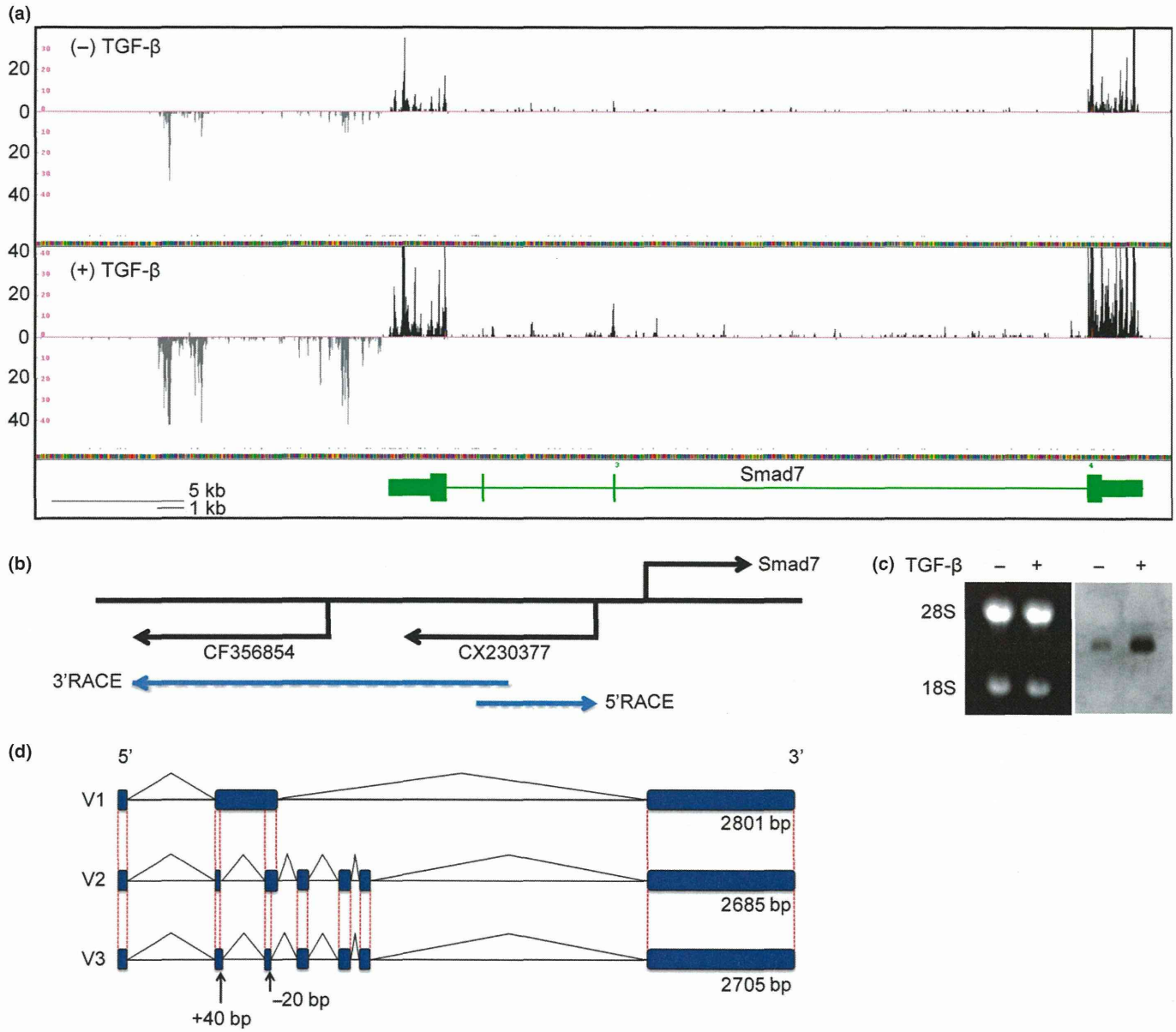

Fig. 1. Cloning of lncRNA-Smad7. (a) RNA-sequencing data from NMuMG cells at the mouse *Smad7* gene locus. Black and grey tags are aligned to the sense and antisense genomic sequences, respectively. Vertical axis: mapped tag numbers. *Smad7* gene is shown in green, and its exons are shown as boxes (thin boxes, untranslated regions; thick boxes, coding regions) connected by horizontal lines representing introns. (b) Relative positions of the *Smad7* gene and EST clones with direction of transcription. Positions of the gene-specific primers used for RACE are shown at the back ends of the blue arrows. (c) Northern blotting of lncRNA-Smad7. NMuMG cells were treated with TGF-β or left untreated for 24 h. Left panel: Ethidium bromide staining of the gel to show the positions of 28s/18s rRNA and equal loading of the samples. Right panel: Northern blotting with an EST sequence (CX230377) as a probe. (d) Schematic representation of the identified lncRNA-Smad7 transcripts. V3 transcript was identified by quantitative RT-PCR (qRT-PCR) analysis of JygMC(A) and confirmed by sequencing of the PCR product. V3 had a longer exon 2 and a shorter exon 3 than V2 transcript.

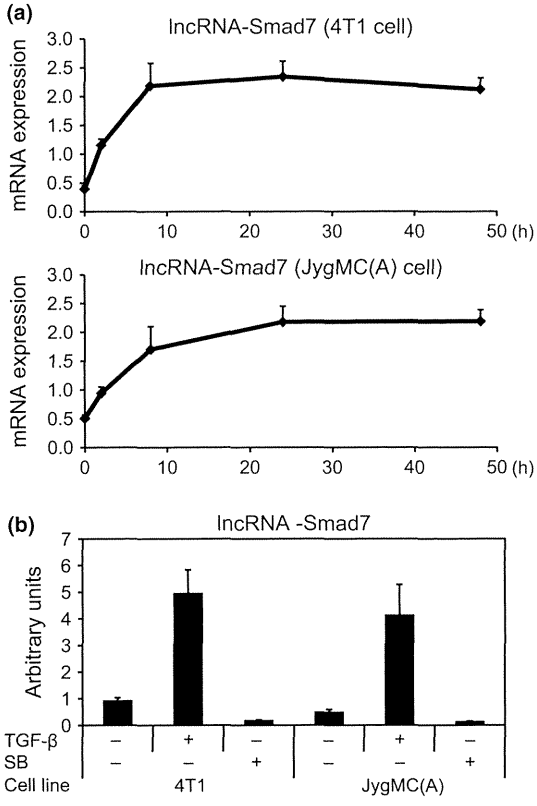

Fig. 2. Upregulation of expression of lncRNA-Smad7 by TGF-β. (a) Effect of TGF-β on expression of lncRNA-Smad7 in mouse JygMC(A) and 4T1 breast cancer cells. Cells were treated with 1 ng/mL TGF-β for the indicated periods, and expression of lncRNA-Smad7 relative to that of TATA box binding protein (Tbp) was determined by quantitative RT-PCR (qRT-PCR). (b) Effect of TGF-β and the TGF-β type I receptor kinase inhibitor SB431542 (SB) on lncRNA-Smad7 expression. Cells were treated with 1 ng/mL TGF-β or 10 μM SB431542 for 48 h or left untreated. Relative expression of lncRNA-Smad7 was determined as in (a). Error bars: standard deviations.

Franklin Lakes, NJ, USA.), rabbit anti-PARP (Cell Signaling Technology), mouse anti-E-cadherin (BD Biosciences), mouse anti-N-cadherin (BD Biosciences) and rabbit anti-fibronectin (Sigma-Aldrich).

Northern blotting. A specific probe to detect lncRNA-Smad7 was made with the DIG T7 RNA Labeling Kit (Roche Diagnostics, Rotkreuz, Risch, Switzerland.) using an EST sequence (CX230377), which was cloned into pBlueScript SK vector as a template. Northern blotting was performed with the DIG Northern Starter Kit (Roche Diagnostics). The probed membrane was washed twice with 2 × SSC (300 mM NaCl, 30 mM sodium citrate, pH 7.0) with 0.1% SDS for 5 min at room temperature and twice with 0.1 × SSC with 0.1% SDS for 15 min at 68°C. HRP-conjugated anti-digoxigenin was used to detect the hybridized probe by chemiluminescent imaging with a lumino-image analyzer (LAS-4000 [GE Health Care, Hino, Tokyo, Japan]).

Rapid amplification of cDNA ends. 5′ and 3′ rapid amplification of cDNA ends (RACE) were performed using the SMARTer RACE cDNA Amplification Kit (TakaraBio, Otsu, Shiga, Japan.) in accordance with the manufacturer's protocol. Gene-specific primers used for 5′ and 3′ RACE were CAGTGCCGTGGA GACCAGAAGAATCCAG and CTGGATTCTTCTGGTCTCCA CGGCACTG, respectively. Following the identification of the 5′ or 3′ ends of the RACE transcripts, we obtained clones of the expected size for lncRNA-Smad7 by PCR using a set of primers designed to hybridize to each end of the transcript.

Immunoprecipitation and immunoblotting. Lysis buffer (1% NP-40, 150 mM NaCl, 50 mM Tris-HCl pH 8.0, 5 mM EDTA and cOmplete EDTA-free protease inhibitor cocktail [Roche Diagnostics]) was used for cell lysis. SDS-gel electrophoresis and immunoblotting were performed as described previously,[13] using the LAS-4000. Quantification of the immunoblotting images was performed using Image-J software (National Institute of Health, Bethesda, MD, USA).

Adenoviral expression vectors. Ad-LacZ and Ad-lncRNA-Smad7 (variant 1) were prepared using the pAd-CMV-V5 vector (TakaraBio). Crude viral lysate was purified using ViraKit Adeno 4 (VIRAPUR, San Diego, CA, USA). Titration was performed with the Adeno-X Rapid Titer Kit (BD Biosciences).

RNA interference. We used two different siRNA against lncRNA-Smad7 (1: 5′-AAGAGUUGGAGUCCGCCAAACUA GG-3′ and 2: 5′-GGGAAGAAGACAGCAGUCAAGAAGA-3′) designed with the BLOCK-iT RNAi Designer (Life Technologies, Carlsbad, CA, USA). Control siRNA was purchased from Life Technologies (Cat. 12935–112, sequence not available). siRNA were introduced into JygMC(A) cells with Lipofectamine 2000 reagent (Life Technologies) according to the manufacturer's instructions. The final concentration of siRNA in the culture medium was 60 nM.

RNA sequencing. Total RNA (10 μg) was purified from NMuMG cells either stimulated with TGF-β or left untreated for 24 h and then polyA selected with Dynabeads Oligo(dT)25 (Life Technologies). Libraries were made and directionally sequenced with the Illumina Genome Analyzer IIx. One lane of the Illumina flow cell was used for each library to obtain sequencing data. Sequenced read tags were directionally aligned to either mm9 transcripts or to the reported genomic loci of lncRNA (mm9)[14] by TopHat2,[15] and differential gene expression calls were performed with the Cuffdiff function of Cufflinks.[16] Note that the reported lncRNA formed multi-exonic structures that were not fully defined. Therefore, we counted all of the mapped tags in the correct direction on each gene locus for the calculation above. The resultant "fragments per kilobase of exon per million mapped fragments sequenced" (FPKM) values thus potentially contain the sequence tags mapped to introns.

Apoptosis assay. Cells were treated as described previously.[4,5] The method is outlined in detail in the online Supporting Information.

Phalloidin staining. Phalloidin staining was performed as described with modification (available in online Supporting Information).[17]

Tumor xenograft assay. Four-week-old female Balb/c nude mice were inoculated subcutaneously with 1.0×10^7 siRNA-transfected JygMC(A) cells. Tumor volume was measured every other day and calculated using the following formula: ([major axis] × [minor axis]^2)/2. All animal experiments were performed in accordance with the policies of the animal ethics committee of the University of Tokyo.

Statistical analysis. Repeated measures ANOVA was used for tumor xenograft assay. The Tukey–Kramer test was used for multiple data comparisons.

Accession numbers. Full nucleotide sequences of lncRNA-Smad7 are available from the DNA Data Bank of Japan (AB904933 and AB904934).

Method for RNA isolation, quantitative real-time PCR and primer sequences for quantitative RT-PCR (qRT-PCR) are available from the online Supporting Online.

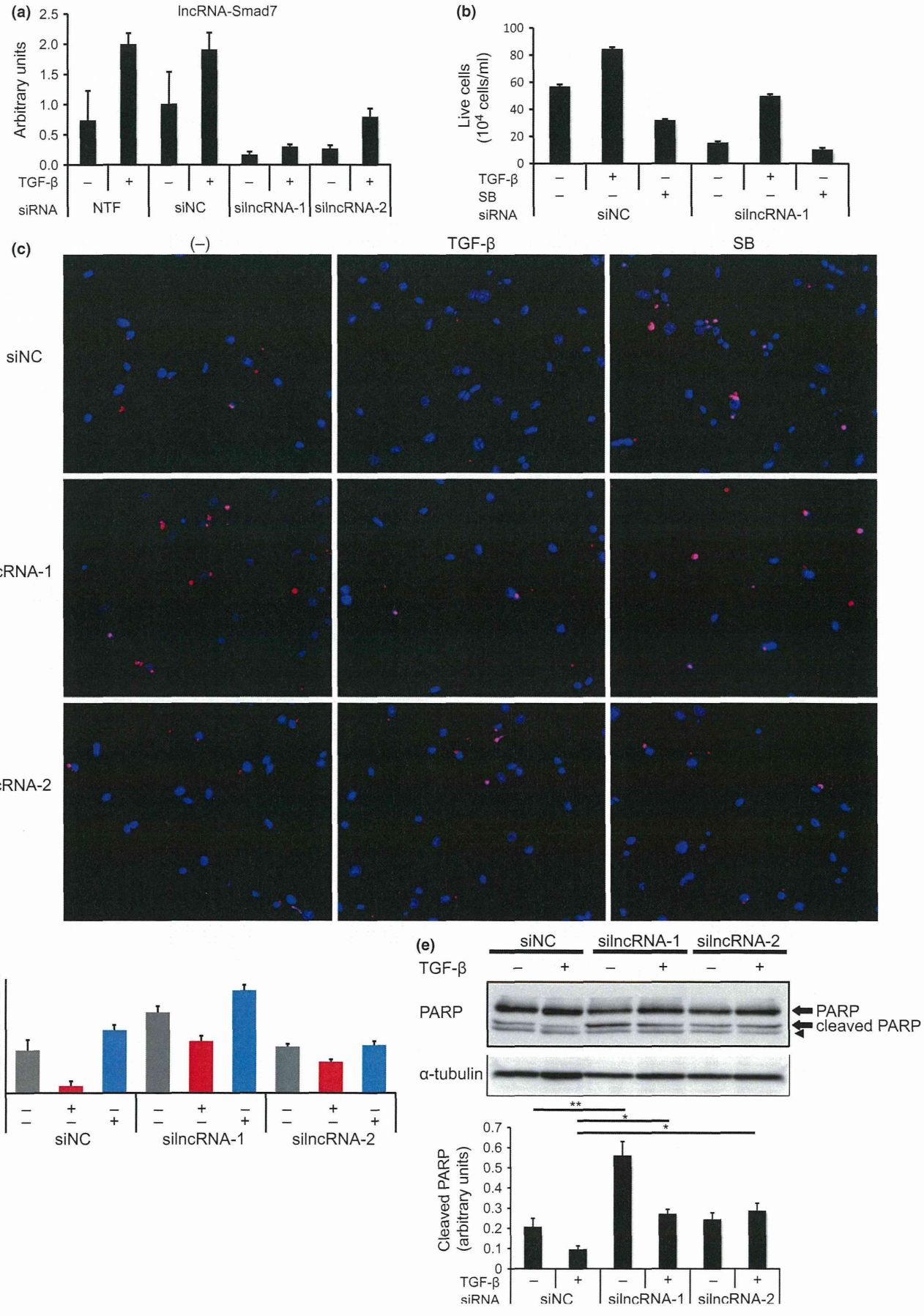

Fig. 3. Knockdown of lncRNA-Smad7 induces apoptosis of JygMC(A) cells. (a) Effect of siRNA for lncRNA-Smad7 in JygMC(A) cells. Cells were transfected with the indicated siRNA and stimulated with 1 ng/mL TGF-β for 48 h after transfection. silncRNA-1 was used for knockdown of all variants of lncRNA-Smad7, while silncRNA-2 was designed for knockdown of V1 only. Relative expression of lncRNA was determined as in Figure 2a. NTF, no transfection control; siNC, negative control siRNA. (b) Live-cell counting of JygMC(A) cells treated with siRNA for lncRNA-Smad7. Cells were transfected with siRNA as indicated and treated with 1 ng/mL TGF-β or 10 μM SB431542 with serum starvation 48 h after transfection. Live cells were counted using TC20 (BioRad, Hercules, California, USA.) after 48 h. (c) TUNEL staining of JygMC(A) cells treated with siRNA for lncRNA-Smad7. Cells were treated as in (b). TUNEL, red; DAPI, blue. (d) The percentage of TUNEL-positive cells among DAPI-positive cells was determined. (e) Immunoblot analysis of cleaved PARP. Cells were treated as in (b) and lysed for SDS-PAGE. An arrow head shows nonspecific band. The graph in the bottom shows quantification of cleaved PARP normalized to α-tubulin. Error bars: standard deviations. $*P < 0.05$, $**P < 0.001$.

Results

Identification of lncRNA-Smad7 as a target gene of transforming growth factor-β. We performed RNA sequencing to quantitatively screen for lncRNA downstream of TGF-β signaling in NMuMG cells. To this end, we calculated changes in the expression of the reported lncRNA after the cells were treated with TGF-β (Table S1).[14] We focused on a TGF-β-induced and highly expressed lncRNA transcribed from an upstream and antisense strand of the *Smad7* gene, which encodes a known target and inhibitor of TGF-β signaling (Fig. 1a). Distribution of the sequenced tags fell within two spliced EST, CX230377 and CF356854, and did not overlap with *Smad7* (Fig. 1b). Northern blotting using CX230377 as a probe resulted in the detection of an approximately 3-kb transcript that was strongly induced by TGF-β treatment (Fig. 1c). We then cloned the transcript by RACE using gene-specific primers designed from CX230377 sequences and identified two transcripts, which we designated lncRNA-Smad7 V1 (2685 bp) and V2 (2801 bp) (Fig. 1d). In addition, variant 3 of lncRNA-Smad7 (V3) was identified through RT-PCR analysis of JygMC(A) cells (data not shown). There were only short open reading frames (ORF) encoding <97 amino acids in lncRNA-Smad7. These ORF did not have a canonical Kozak sequence (data not shown).

We next analyzed the expression of lncRNA-Smad7 in 4T1 and JygMC(A) mouse breast cancer cells by qRT-PCR.

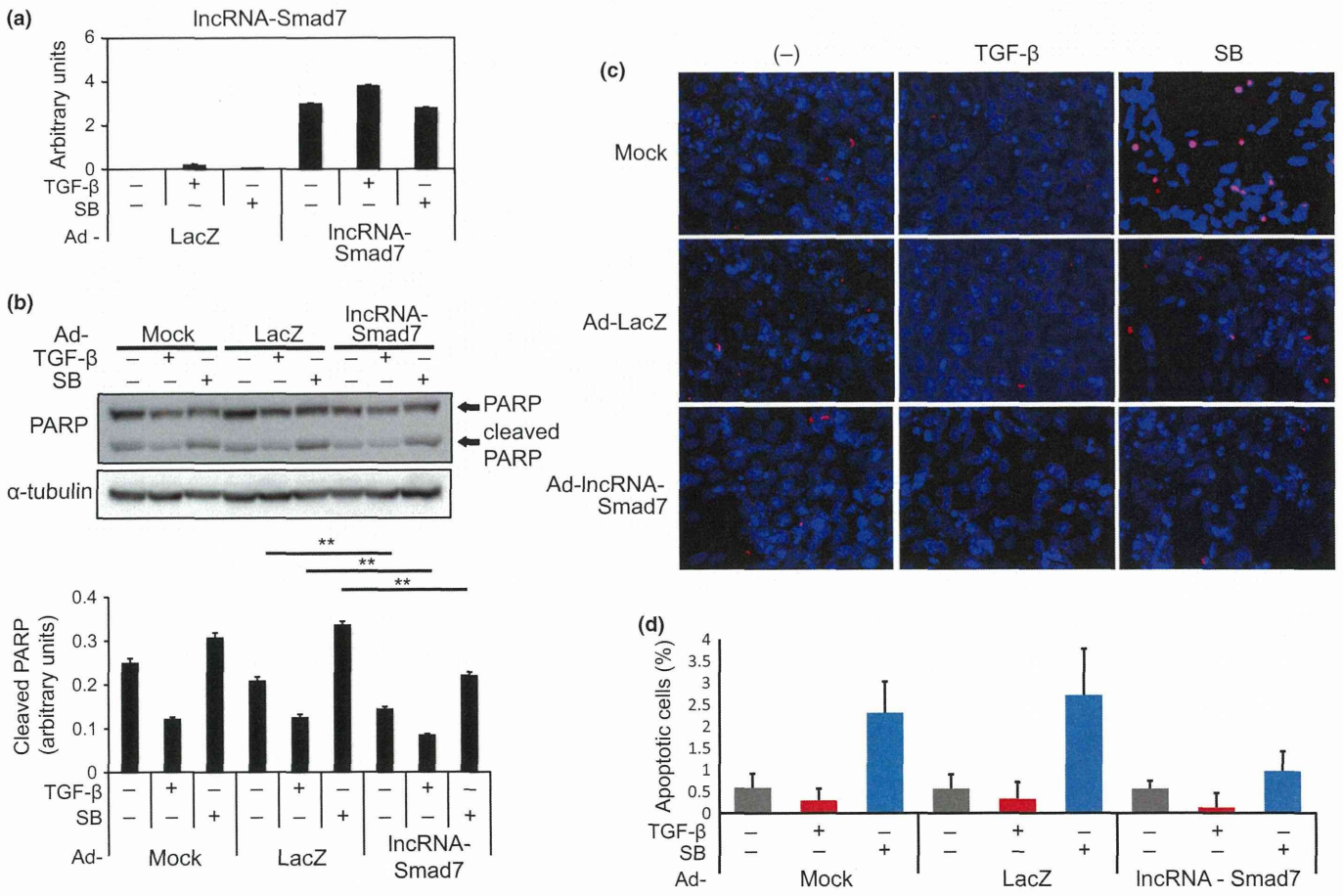

Fig. 4. Forced expression of lncRNA-Smad7 partially inhibits apoptosis of JygMC(A) cells. (a) Cells were infected with either adenoviral lncRNA-Smad7 expression vector (Ad-lncRNA-Smad7) or Ad-LacZ as a control. Twelve hours after infection, cells were serum starved and treated with 1 ng/mL TGF-β or 10 μM SB431542 (SB) for 48 h. Expression of lncRNA-Smad7 was determined by quantitative RT-PCR (qRT-PCR). (b) Effect of Ad-lncRNA-Smad7 on cleaved PARP level was determined by immunoblotting. Cells were treated as in (a) and lysed for SDS-PAGE. The bottom graph shows quantification of cleaved PARP normalized to α-tubulin. $**P < 0.001$. (c) TUNEL staining of JygMC(A) cells. Cells were treated as in (a). TUNEL, red; DAPI, blue. (d) The percentage of TUNEL-positive cells among DAPI-positive cells was determined. Error bars: standard deviations.

Expression of lncRNA-Smad7 was induced early after stimulation with TGF-β and continued for 48 h (Fig. 2a). Upregulation of lncRNA-Smad7 by TGF-β was observed in two other mouse mammary gland cell lines, EpH4 and EpRas (Fig. S1). Both 4T1 and JygMC(A) cells secrete endogenous TGF-β,[5] and basal expression of lncRNA-Smad7 was inhibited by the TGF-β type I receptor kinase inhibitor SB431542 (Fig. 2b). These results suggest that lncRNA-Smad7 is expressed in several mouse mammary gland epithelial cell lines and that TGF-β upregulates its expression in breast cancer cells.

lncRNA-Smad7 inhibits apoptosis of breast cancer cells induced by transforming growth factor-β. We next knocked down the expression of lncRNA-Smad7 by two different siRNA; that is, silncRNA-1 and silncRNA-2 (Fig. 3a). silncRNA-1 was designed to knock down all three variants, while silncRNA-2 was designed to knock down only V1. As shown in Figure 3a, expression of lncRNA-Smad7 was repressed efficiently by silncRNA-1 and moderately by silncRNA-2 in JygMC(A) cells. We found that live cell counts were decreased by silncRNA-1 *in vitro* (Fig. 3b). JygMC(A) cells underwent apoptosis upon serum starvation, and the apoptosis was induced by SB431542 and inhibited by TGF-β.[4] The role of lncRNA-Smad7 in TGF-β-induced anti-apoptosis was then evaluated. Inhibition of apoptosis by TGF-β was partially cancelled by suppression of lncRNA-Smad7 expression, as determined by TUNEL staining (Fig. 3c,d). Consistent with the silencing efficiencies, the effects of silncRNA-2 were less marked than those of silncRNA-1 (Fig. 3c,d). Cleaved PARP levels in TGF-β-stimulated cells were also increased following treatment with silncRNA-1 and silncRNA-2 (Fig. 3e).

The adenoviral lncRNA-Smad7 expression vector (Ad-lncRNA-Smad7) was then constructed to examine its effect on apoptosis. Expression of exogenous lncRNA-Smad7 was confirmed by qRT-PCR and compared with endogenous expression levels and with a sample without reverse transcription (Fig. 4a and data not shown). Partial inhibition by Ad-lncRNA-Smad7 of cleaved PARP expression was observed in both TGF-β-stimulated and TGF-β-unstimulated cells (Fig. 4b). The numbers of TUNEL-positive cells induced by SB431542 treatment were reduced by forced expression of lncRNA-Smad7 (Fig. 4c,d), which suggests that lncRNA-

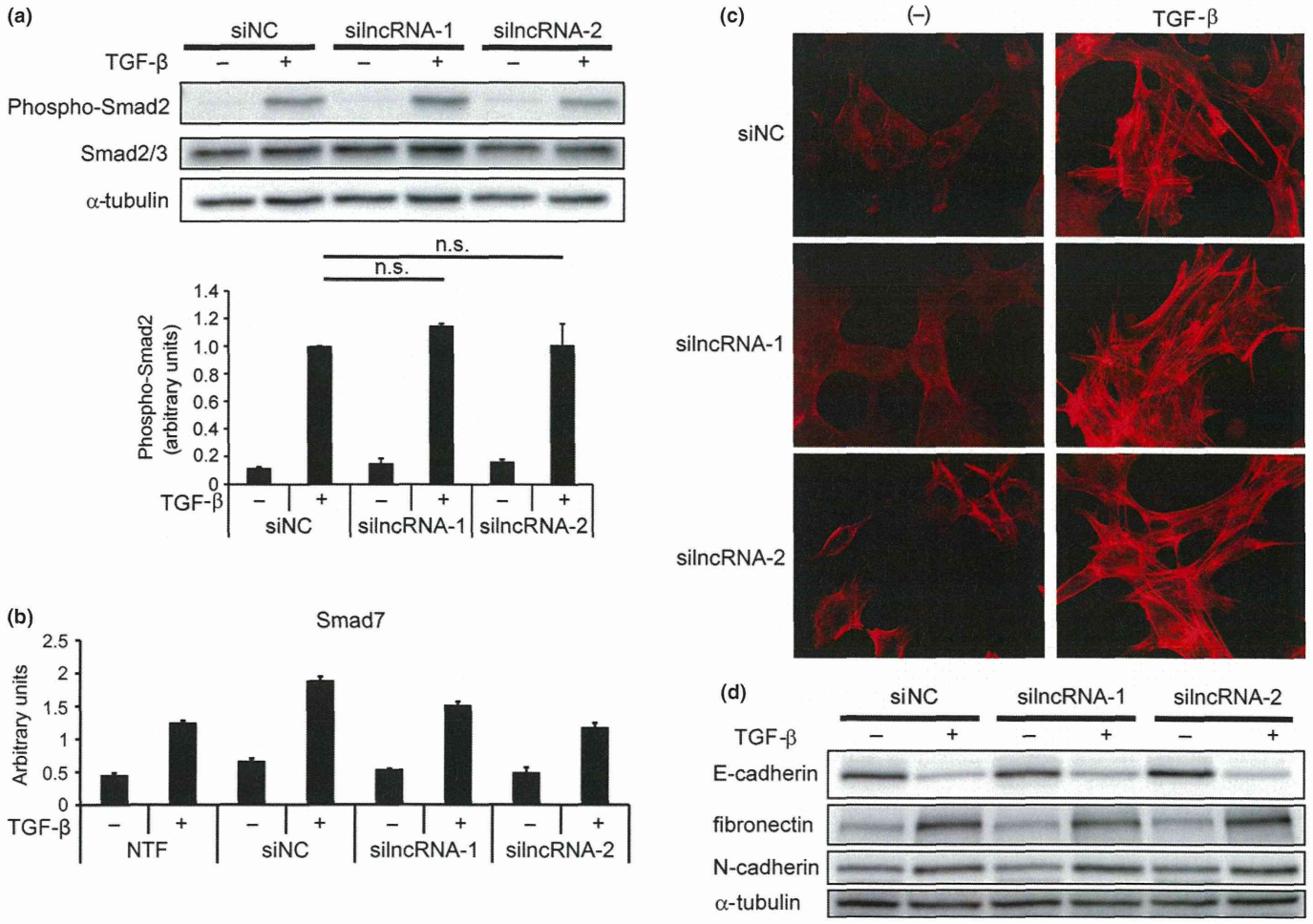

Fig. 5. lncRNA-Smad7 does not regulate phospho-Smad2 levels or TGF-β-induced EMT. (a) JygMC(A) cells were transfected with siRNA as indicated and stimulated with TGF-β for 48 h. Phospho-Smad2 and total Smad2/3 levels were determined by immunoblotting (top panel). The bottom graph shows quantification of phospho-Smad2 normalized to total Smad2/3. n.s.: not significant. (b) Effect of siRNA for lncRNA-Smad7 on Smad7 expression evaluated by quantitative RT-PCR (qRT-PCR). Transfected cells were stimulated with TGF-β for 48 h. NTF, no transfection; error bars, standard deviations. (c) NMuMG cells were reverse-transfected with siRNA as indicated. Twelve hours later, cells were stimulated with TGF-β for 24 h and fixed. F-actin formation was evaluated by phalloidin staining. (d) NMuMG cells were treated as in (c) and expression of EMT marker proteins was determined by immunoblotting.

Smad7 acts as an anti-apoptotic factor downstream of TGF-β signaling.

Effect of lncRNA-Smad7 on transforming growth factor-β-Smad signaling pathway and transforming growth factor-β-induced epithelial–mesenchymal transition. lncRNA have several modes of function, including neutralizing miRNA and inhibiting transcription of target genomic regions.[8] Therefore, we next evaluated the effect of siRNA for lncRNA-Smad7 on the TGF-β-Smad signaling pathway. Knockdown of lncRNA-Smad7 did not change phospho-Smad2 expression in JygMC(A) cells (Fig. 5a). Moreover, expression of Smad7 by TGF-β stimulation was minimally inhibited by the siRNA for lncRNA-Smad7 (Fig. 5b). We then evaluated the effect of silncRNA on TGF-β-induced EMT in NMuMG cells. Actin stress fiber formation by TGF-β stimulation was not inhibited by the silncRNA, and silncRNA-2 showed a mild F-actin-inducing effect in the absence of TGF-β (Fig. 5c). Both downregulation of E-cadherin and induction of fibronectin and N-cadherin by TGF-β were not affected by the silncRNA (Fig. 5d). These results suggest that lncRNA-Smad7 does not have a marked effect on TGF-β signaling in general but does regulate anti-apoptosis-specific effects. Upregulation of *Bhlhe40* (encoding the anti-apoptotic DEC1 protein) and inhibition of *Bcl2l11* (encoding the pro-apoptotic BH3-only protein Bim) through downregulation of Foxc1 have been demonstrated as mechanisms of TGF-β-induced anti-apoptosis in breast cancer cells.[4,5] We examined the effect of lncRNA-Smad7 on the mRNA levels of these molecules, but the changes in their expression profiles could not explain the anti-apoptotic function of lncRNA-Smad7 (Fig. S2). We also searched for other pro-apoptotic and anti-apoptotic factors whose mRNA and protein expression levels were regulated by lncRNA-Smad7, but we were not able to identify any definite targets (data not shown).

Role of lncRNA-Smad7 in xenografted tumor formation. Finally, we examined whether lncRNA-Smad7 affects the tumor-forming ability of JygMC(A) cells. Tumor size was periodically measured after subcutaneous inoculation of siRNA-transfected JygMC(A) cells into mice. As shown in Figure 6, knockdown of lncRNA-Smad7 resulted in reduced tumor size, suggesting impaired graft survival in the absence of lncRNA-Smad7 (Fig. 6a,b).

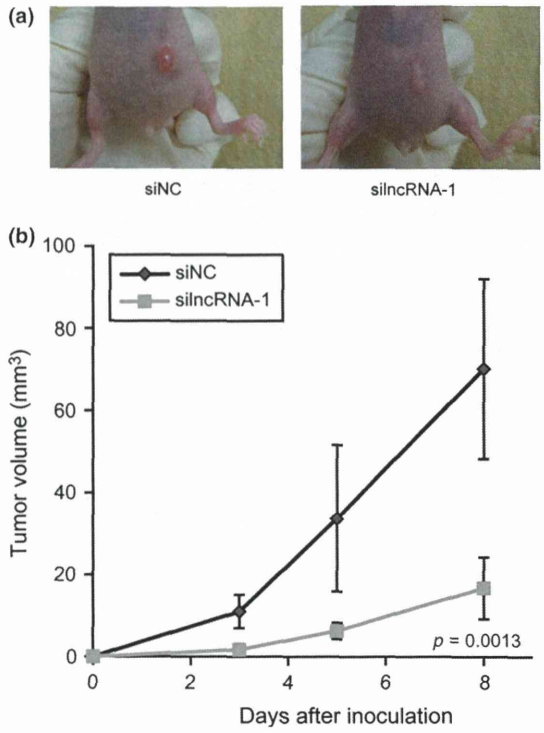

Fig. 6. Knockdown of lncRNA-Smad7 represses tumor-forming ability of JygMc(A) cells. (a) Effect of siRNA for lncRNA-Smad7 (silncRNA-1) on the size of xenografted tumors ($n = 6$). Photos were taken 8 d after tumor inoculation. Representative images are shown in this figure. (b) Sequential tumor volume measurement after inoculation. Error bars: standard deviations.

Discussion

In the present study, we identified lncRNA-Smad7 through a search for TGF-β-regulated transcripts in mouse mammary NMuMG cells. lncRNA-Smad7 is located adjacent to the mouse *Smad7* gene and is strongly upregulated by TGF-β in the mouse mammary gland epithelial cells and mouse breast cancer cells. lncRNA-Smad7 appears to function as a downstream anti-apoptotic factor of TGF-β in the mouse breast cancer cell line JygMC(A) without affecting activation of Smad2 and induction of EMT.

lncRNA regulate gene expression through several mechanisms in cancer.[18] The lncRNA HOTAIR was identified in breast tumors as a poor prognosis marker that induces alteration of Polycomb-regulated histone H3K27 modification and gene expression.[10,19] Subsequently, the presence of HOTAIR was reported to be associated with the prognosis of nasopharyngeal carcinoma and esophageal cancer.[20,21] Zhang *et al.*[22] reported that the lncRNA-RoR inhibited translation of p53 and apoptosis in MCF-7 breast cancer cells. Importantly, lncRNA-RoR also functions as a miRNA sponge to inhibit a set of miRNA in human ES cells, suggesting that even a single type of lncRNA has several modes of action.[23] Other lncRNA are related to the pathogenesis of breast cancers. The ATM target gene lncRNA-JADE protects MCF7 cells from several DNA-damaging drugs to maintain tumor formation.[24] In addition, Hu *et al.*[25] analyzed lncRNA expression signatures during the twist-induced EMT of MCF10A cells.

We identified lncRNA-Smad7 as a new anti-apoptosis factor in mouse breast cancer cells, although we could not identify the regulatory mechanism of apoptosis induced by lncRNA-Smad7. In principle, siRNA-based loss-of-function analyses of lncRNA may not be an ideal means of evaluating their transcriptional or epigenomic regulatory mechanisms. Therefore, we cannot conclude that lncRNA-Smad7 does not regulate transcription of the adjacent *Smad7* and other genes. In contrast, the anti-apoptotic activity of lncRNA-Smad7 observed in our siRNA experiments could instead be executed through post-transcriptional regulatory mechanisms. Determining the effect of lncRNA-Smad7 on Smad7 expression will be an important topic for future analysis, because Smad7 sensitizes MCF7 cells to IRF1-induced apoptosis.[26]

Our present analysis revealed that lncRNA-Smad7 was widely expressed in mouse mammary epithelial cells and mouse breast cancer cells. This transcript was previously found in a list yielded by transcriptome analyses of mouse ES cells,[14] suggesting that it is broadly expressed in many mouse cell types and tissues. Transcriptional upregulation of lncRNA-Smad7 by TGF-β would also be a general mechanism in mice, because the transcriptional start site of lncRNA-Smad7 is close to Smad7, a well-known target of TGF-β/Smad signaling. Guttman *et al.* included this lncRNA in their loss-of-function screening based on the good conservation among species, and

lncRNA-Smad7 was designated as linc1316 in their list (table 1).[14] However, our efforts to find a human ortholog by using our unpublished RNA-sequencing data from several TGF-β-treated human epithelial cell lines and cancer cell lines were unsuccessful (data not shown). Moreover, a BLAST-based search for lncRNA-Smad7-like genomic sequences showed that only approximately 400 nucleotides out of the 3-kb mouse lncRNA-Smad7 are conserved upstream of *SMAD7* in humans, which was in contrast to the high conservation between mice and rats (data not shown). Therefore, lncRNA-Smad7 appears to be a rodent-specific transcript. However, there is still a possibility that the identified 400-bp region in humans might be transcribed in a limited condition and has functions similar to that of mouse lncRNA-Smad7 in human breast cancers.

Comprehensive analysis of transcriptional regulation of the many target genes of TGF-β through ChIP-sequencing or ChIP-chip analyses have been performed in several cancer cell lines,[27–31] and large-scale transcriptome data from several cancer types are available. In the case of lncRNA, Zhou *et al.*[32] reported a list of TGF-β-Smad3 target lncRNA expressed during renal inflammation and fibrosis. However, the lack of knowledge about the function of non-coding transcripts often limits the utility of these types of data. Our findings, together with the findings of low conservation of lncRNA among species, suggest that determination of the roles of each non-coding transcript is required to understand their relevance to cancer biology.

Acknowledgements

The authors are grateful to Kaori Shiina and Keiko Yuki for technical assistance, as well as to members of the Miyazono Laboratory for discussion and advice. This research was supported by KAKENHI (grants-in-aid for scientific research on Innovative Areas [Integrative Research on Cancer Microenvironment Network; 22112002, K.M.], Scientific Research [S] [20221009, H.A.], [C] [24501311, D.K.] and [B] [24390070, K.M.]) from the Ministry of Education, Culture, Sports, Science and Technology of Japan (MEXT) and a grant from the Ministry of Health, Labor, and Welfare of Japan (D.K.). This study was performed in part as a research program of the Project for Development of Innovative Research on Cancer Therapeutics (P-Direct) from MEXT, and a grant from the Swedish Cancer Foundation (No. 100452, K.M.). D.K. is supported by a grant from the Mochida Memorial Foundation for Medical and Pharmaceutical Research. M.A. is supported by grants from the Ishidsu Shun Memorial Scholarship and the Japan Society for the Promotion of Science. M.M. is supported by the Kanae Foundation for Research Abroad and the ITO Genboku and SAGARA Chian Memorial Scholarship.

Disclosure Statement

The authors have no conflict of interest to declare.

References

1 Happo L, Strasser A, Cory S. BH3-only proteins in apoptosis at a glance. *J Cell Sci* 2012; **125**: 1081–7.
2 Roberts AB, Wakefield LM. The two faces of transforming growth factor-β in carcinogenesis. *Proc Natl Acad Sci USA* 2003; **100**: 8621–3.
3 Miyazono K, Ehata S, Koinuma D. Tumor-promoting functions of transforming growth factor-β in progression of cancer. *Ups J Med Sci* 2012; **117**: 143–52.
4 Ehata S, Hanyu A, Hayashi M *et al.* Transforming growth factor-β promotes survival of mammary carcinoma cells through induction of antiapoptotic transcription factor DEC1. *Cancer Res* 2007; **67**: 9694–703.
5 Hoshino Y, Katsuno Y, Ehata S, Miyazono K. Autocrine TGF-β protects breast cancer cells from apoptosis through reduction of BH3-only protein, Bim. *J Biochem* 2011; **149**: 55–65.
6 Gadir N, Jackson DN, Lee E, Foster DA. Defective TGF-β signaling sensitizes human cancer cells to rapamycin. *Oncogene* 2008; **27**: 1055–62.
7 Okazaki Y, Furuno M, Kasukawa T *et al.* Analysis of the mouse transcriptome based on functional annotation of 60,770 full-length cDNAs. *Nature* 2002; **420**: 563–73.
8 Chen LL, Carmichael GG. Decoding the function of nuclear long non-coding RNAs. *Curr Opin Cell Biol* 2010; **22**: 357–64.
9 Bartolomei MS, Zemel S, Tilghman SM. Parental imprinting of the mouse H19 gene. *Nature* 1991; **351**: 153–5.
10 Gupta RA, Shah N, Wang KC *et al.* Long non-coding RNA HOTAIR reprograms chromatin state to promote cancer metastasis. *Nature* 2010; **464**: 1071–6.
11 Yan B, Wang Z. Long noncoding RNA: its physiological and pathological roles. *DNA Cell Biol* 2012; **31**(Suppl. 1): S34–41.
12 Serpico D, Molino L, Di Cosimo S. MicroRNAs in breast cancer development and treatment. *Cancer Treat Rev* 2014; **40**: 595–604.
13 Mizutani A, Saitoh M, Imamura T, Miyazawa K, Miyazono K. Arkadia complexes with clathrin adaptor AP2 and regulates EGF signalling. *J Biochem* 2010; **148**: 733–41.
14 Guttman M, Donaghey J, Carey BW *et al.* lincRNAs act in the circuitry controlling pluripotency and differentiation. *Nature* 2011; **477**: 295–300.
15 Kim D, Pertea G, Trapnell C, Pimentel H, Kelley R, Salzberg SL. TopHat2: accurate alignment of transcriptomes in the presence of insertions, deletions and gene fusions. *Genome Biol* 2013; **14**: R36.
16 Trapnell C, Roberts A, Goff L *et al.* Differential gene and transcript expression analysis of RNA-seq experiments with TopHat and Cufflinks. *Nat Protoc* 2012; **7**: 562–78.
17 Shirakihara T, Saitoh M, Miyazono K. Differential regulation of epithelial and mesenchymal markers by δEF1 proteins in epithelial mesenchymal transition induced by TGF-β. *Mol Biol Cell* 2007; **18**: 3533–44.
18 Gutschner T, Diederichs S. The hallmarks of cancer: a long non-coding RNA point of view. *RNA Biol* 2012; **9**: 703–19.
19 Chu C, Qu K, Zhong FL, Artandi SE, Chang HY. Genomic maps of long noncoding RNA occupancy reveal principles of RNA-chromatin interactions. *Mol Cell* 2011; **44**: 667–78.
20 Nie Y, Liu X, Qu S, Song E, Zou H, Gong C. Long non-coding RNA HOTAIR is an independent prognostic marker for nasopharyngeal carcinoma progression and survival. *Cancer Sci* 2013; **104**: 458–64.
21 Ge XS, Ma HJ, Zheng XH *et al.* HOTAIR, a prognostic factor in esophageal squamous cell carcinoma, inhibits WIF-1 expression and activates Wnt pathway. *Cancer Sci* 2013; **104**: 1675–82.
22 Zhang A, Zhou N, Huang J *et al.* The human long non-coding RNA-RoR is a p53 repressor in response to DNA damage. *Cell Res* 2013; **23**: 340–50.
23 Wang Y, Xu Z, Jiang J *et al.* Endogenous miRNA sponge lincRNA-RoR regulates Oct4, Nanog, and Sox2 in human embryonic stem cell self-renewal. *Dev Cell* 2013; **25**: 69–80.
24 Wan G, Hu X, Liu Y *et al.* A novel non-coding RNA lncRNA-JADE connects DNA damage signalling to histone H4 acetylation. *EMBO J* 2013; **32**: 2833–47.
25 Hu P, Yang J, Hou Y *et al.* LncRNA expression signatures of twist-induced epithelial-to-mesenchymal transition in MCF10A cells. *Cell Signal* 2014; **26**: 83–93.
26 Hong S, Kim HY, Kim J *et al.* Smad7 protein induces interferon regulatory factor 1-dependent transcriptional activation of caspase 8 to restore tumor necrosis factor-related apoptosis-inducing ligand (TRAIL)-mediated apoptosis. *J Biol Chem* 2013; **288**: 3560–70.
27 Zhang Y, Handley D, Kaplan T *et al.* High throughput determination of TGF-β1/SMAD3 targets in A549 lung epithelial cells. *PLoS ONE* 2011; **6**: e20319.
28 Mizutani A, Koinuma D, Tsutsumi S *et al.* Cell type-specific target selection by combinatorial binding of Smad2/3 proteins and hepatocyte nuclear factor 4α in HepG2 cells. *J Biol Chem* 2011; **286**: 29848–60.
29 Kennedy BA, Deatherage DE, Gu F *et al.* ChIP-seq defined genome-wide map of TGF-β/SMAD4 targets: implications with clinical outcome of ovarian cancer. *PLoS ONE* 2011; **6**: e22606.
30 Qin H, Chan MW, Liyanarachchi S *et al.* An integrative ChIP-chip and gene expression profiling to model SMAD regulatory modules. *BMC Syst Biol* 2009; **3**: 73.
31 Morikawa M, Koinuma D, Miyazono K, Heldin CH. Genome-wide mechanisms of Smad binding. *Oncogene* 2013; **32**: 1609–15.
32 Zhou Q, Chung AC, Huang XR, Dong Y, Yu X, Lan HY. Identification of novel long noncoding RNAs associated with TGF-β/Smad3-mediated renal inflammation and fibrosis by RNA sequencing. *Am J Pathol* 2014; **184**: 409–17.

Supporting Information

Additional supporting information may be found in the online version of this article:

Table S1. lncRNA regulated by transforming growth factor (TGF)-β

Fig. S1. Upregulation of lncRNA-Smad7 in mouse mammary gland cell lines.

Fig. S2. Effects of siRNA for lncRNA-Smad7 on expression of DEC1 and Bim.

Pathology International

Pathology International 2014; **64**: 292–294 doi:10.1111/pin.12160

Letter to the Editor

Plasmacytic ALK-positive large B-cell lymphoma: A potential mimic of extramedullary plasmacytoma

To the Editor:

ALK-positive large B-cell lymphoma (ALK+ LBCL) is defined as a B-cell neoplasm that expresses the ALK protein.[1] This lymphoma occurs in all age groups with a male predominance (M:F ratio, 3:1). Although the tumor mainly involves lymph nodes, the involvement of various extranodal sites including the gastrointestinal (GI) tract, ovaries, nasopharynx, tongue, brain, liver, bone and spleen has been reported.[1,2] Most patients with ALK+ LBCL present with an advanced stage and have an aggressive course and a poor prognosis.[1] The diagnosis of ALK+ LBCL can be challenging because ALK analysis is not performed routinely in clinical practice. The inclusion of ALK+ LBCL in differential diagnosis is essential to reach a correct diagnosis. Histologically, the neoplastic cells are medium-sized to large, having immunoblast-like nuclei which is characterized by centrally located conspicuous nucleoli, with positive plasmacytic markers (e.g. CD138, CD38) without expressing usual B-cell-lineage markers (e.g. CD19, CD20), which are interpreted as plasmablastic.[1] Thus, the main histological differential diagnoses of ALK+ LBCL are aggressive lymphomas with immunoblastic or plasmablastic morphology. Here, we report a case of ALK+ LBCL, which was a diagnostic challenge due to its low grade atypia. The tumor cells were plasmacytic, having abundant amphophilic cytoplasm, eccentrically located round nuclei with coarse chromatin, and perinuclear halo. Nucleoli were inconspicuous in the majority of the tumor cells and it simulated extramedullary plasmacytoma (EMP).

A previously healthy 31-year-old woman presented with a 1-month history of lower abdominal pain. Physical examination revealed a soft palpable mass of the umbilical to lower abdominal area with tenderness. There was no apparent lymph node swelling. Laboratory data included lactate dehydrogenase (LDH) level of 262 IU/L (normal range, 129–241 IU/L), CA 125 level of 111.2 U/mL (normal range, less than 35 U/mL) and soluble interleukin-2 receptor (sIL-2R) level of 391 U/mL (normal range, 145–519 U/mL). Magnetic resonance imaging (MRI) showed an abdominal mass (about 5 cm in greatest diameter), thickening of the greater omentum and multiple disseminated nodules. Positron emission tomographic/computed tomographic study revealed the accumulation of fluorodeoxyglucose within these areas. On suspicion of ovarian cancer, open biopsy of the peritoneal nodule was performed. Finally, the patient was diagnosed as stage IVB lymphoma confined to the abdominal cavity and underwent three cycles of hyper-CVAD/HD-MTX-Ara-C (cyclophosphamide, vincristine, doxorubicin, dexamethasone, high-dose methotrexate, cytarabine) therapy. Restaging PET-CT study revealed complete remission. The patient subsequently underwent autologous peripheral blood stem cell transplantation using a MEAM (ranimustine, etoposide, cytarabine, melphalan) conditioning regimen. She is alive and disease-free 2 years later.

Intraoperative histological evaluation of frozen section of the abdominal tumor showed somewhat cohesive proliferation of atypical cells and poorly differentiated carcinoma was suspected. Flow cytometry and chromosomal analysis were not performed. Final paraffin section showed a diffuse infiltrate of plasmacytic tumor cells with abundant amphophilic cytoplasm, eccentric nuclei with coarse chromatin and perinuclear clearing (Fig. 1a). The immunophenotype was also plasmacytic; CD4 (SP35, Roche Diagnostics, Indianapolis, IN, USA), CD56 (1B6, Novocastra, Newcastle, UK), CD138 (B-A38, Roche Diagnostics), EMA (E29, Dako, Carpinteria, CA, USA), Ig kappa (polyclonal Roche Diagnostics), and MUM-1 (MUM1p, Dako) were positive; AE1/AE3 (AE1/3/PCK26, Roche Diagnostics), CD3 (2GV6, Roche Diagnostics), CD5 (4C7, Novocastra), CD8 (C8144B, Dako), CD20 (L26, Dako), CD30 (Ber-H2, Dako), CD79a (JCB117, Dako), Cyclin D1 (SP4, Neomarkers, Fremont, CA, USA), HHV-8 (Rat ORF73, Advanced Biotechnologies, Columbia, MD, USA), Ig lambda (polyclonal, Roche Diagnostics), PAX5 (polyclonal, Thermo Scientific, Rockford, IL, USA), and TIA-1 (2G9, Beckman Coulter, Brea, CA, USA) were negative. All immunostains were performed on an autoimmunostainer, Ventana XT system benchmark. Plasmablastic cells were observed, but only in about 10% of the total tumor cells (Fig. 1b) and the Ki-67 (MIB-1, Dako) labeling index (≒40%) was low for plasmablastic lymphoma (Fig. 1c).[1] In addition, *in situ* hybridization for EBV-encoded RNA (Inform EBER probe; Roche Diagnostics) was negative. Histologically, plasmacytoma seemed the most likely diagnosis; however, an unusual site of involvement and focal plasmablastic feature prompted us to perform ALK immunostaining (p80SP8, Thermo Scientific, Rockford, IL, USA), which turned out to be positive in the cytoplasm (Fig. 1d). Subsequently, *ALK* split fluorescence *in situ* hybridization (FISH) analysis demonstrated *ALK* gene rearrangement (Fig. 2a) and *SEC31A-ALK* fusion was identified by reverse transcription-polymerase chain reaction (RT-PCR), using the primers *SEC31A-2101F* (5′-tccagccctgctacttctttc-3′) and *ALK3200R* (5′-tgcagctcctggtgcttc-3′), by the methods described in a previous paper using formalin-fixed paraffin-embedded tissue.[3] In the analysis, two different bands of PCR-amplified products at 188 bp and 143 bp were visualized with ethidium

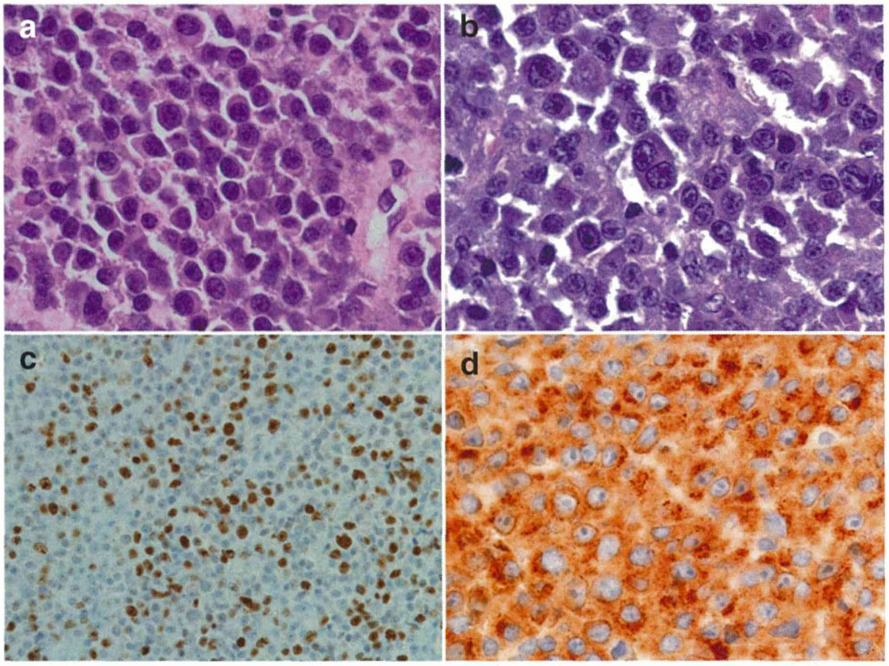

Figure 1 Proliferation of relatively uniform plasmacytic tumor cells that have amphophilic cytoplasm with perinuclear hof and eccentrically located nuclei. (**a**) Plasmablastic morphology was seen, accounting for approximately 10% of total tumor cells. (**b**) About 40% of the lymphoma cells were positive for Ki-67. (**c**) Anaplastic lymphoma kinase stain showed diffuse cytoplasmic granular staining.

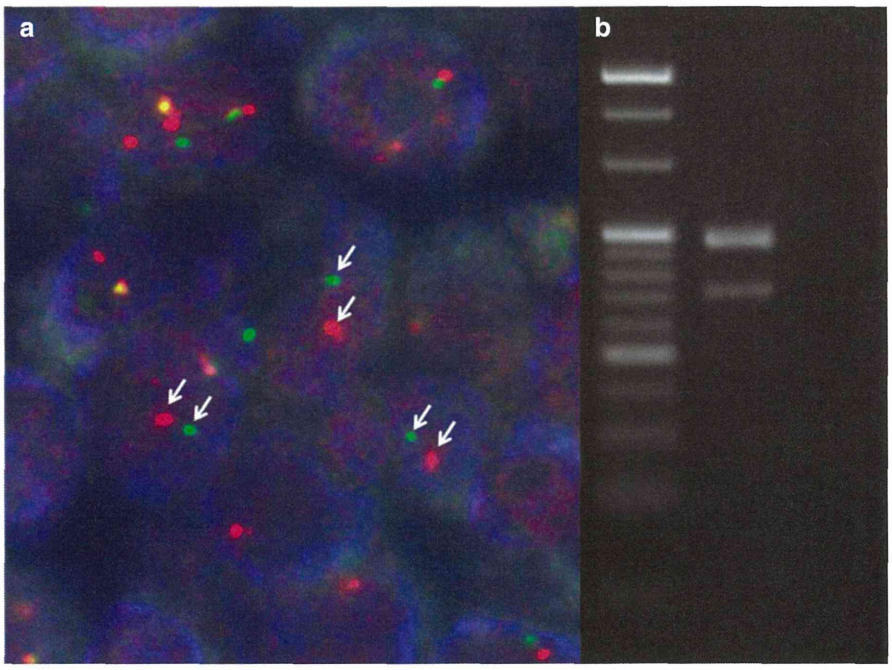

Figure 2 (**a**) Dual-color interphase fluorescent *in situ* hybridization for the detection of breakpoint in the *ALK* locus. Tumor cells with isolated red and green signals are shown, indicating the presence of a breakpoint in the *ALK* locus. (**b**) Polymerase chain reaction-amplified products visualized with ethidium bromide in an ultraviolet-illuminated agarose gel. Left lane, molecular markers. Middle lane, two bands of *SEC31A-ALK* products. Right lane, control with no template.

bromide in an ultraviolet-illuminated agarose gel (Fig. 2b). The sequencing of these PCR products revealed that the higher band of 188 bp had 100% homology with an already described fusion transcript (tccagccctgctacttctttccctcctccc ccttcctctggagcatccttccagcatggcggaccaggagctccaccatcatcttca gcttatgcactgcctcctggaacaacagtgtaccgccggaagcaccaggagctg ca),[4,5] while the lower one was interpreted as a novel splicing variant corresponding to an in-frame deletion of 45 bp in the 3′ end of exon 22 of SEC31A (tccagccctgctacttctttccctcct ccccttcctctggagcatccttccagcatggcggaccaggagtgtaccgccgga agcaccaggagctgca). A final diagnosis of ALK+ LBCL was made from these findings.

ALK+ LBCL shows morphological and immunohistological features that overlap with those of different lymphomas with plasmablastic differentiation, such as plasmablastic lymphoma, LBCL arising in HHV8-associated multicentric Castleman disease and primary effusion lymphoma. In our case, majority of the tumor cells showed rather plasmacytic

morphology than plasmablastic. However, the minor component of plasmablastic tumor cells and unusual clinical presentation for EMP made us examine ALK protein. About 80% of EMP occur in upper respiratory tract and it usually follow indolent clinical course which suggest that many cases are more closely related to extranodal marginal zone lymphoma than to myeloma.[1] There are a few cases of ALK+ LBCL that were initially diagnosed as plasmacytoma in the previous literature.[2,6] It seems to be a rare phenomenon for ALK+ LBCL to reveal evident plasmacytic differentiation;[6] however, it is clinically important to distinguish ALK+ LBCL from EMP because the biological behavior and chemotherapy regimen are quite different. Whether the low-grade morphology in ALK+ LBCL is related to a better prognosis also needs further investigation.

The overexpression of ALK protein is associated with abnormal fusion between *ALK* and other partner genes. There are five known partner genes fused to *ALK* in ALK+ LBCL. The most common is *CLTC-ALK*.[1,6,7] *NPM-ALK*,[4,8] *SEC31A-ALK*,[4,5] *SQSTM1-ALK*,[9] and *RANBP2-ALK*[10] fusions have also been reported. Our case had *SEC31A* gene abnormality, which was unique in the two *SEC31A-ALK* products identified by RT-PCR, probably reflecting the splicing variant of SEC31A. SEC31A is an essential protein for endoplasmic reticulum-Golgi transport, which is mainly distributed in the cytoplasm of mammalian cells. The cytoplasmic staining pattern of ALK in our case may be explained by the regular allocation of the SEC31A protein.[4]

In this report, we described a case of ALK+ LBCL with obvious plasmacytic differentiation. Pathologists should perform appropriate immunohistochemistry including ALK to exclude the possibility of ALK+ LBCL when making a diagnosis of EMP.

Taiki Hashimoto,[1] Masakazu Fujimoto,[1] Momoko Nishikori,[2] Kengo Takeuchi,[3] Mizuki Kimura,[1] Naoki Nakajima,[1] Aya Miyagawa-Hayashino,[1] Akifumi Takaori-Kondo[2] and Hironori Haga[1]

Departments of [1]Diagnostic Pathology and [2]Hematology and Oncology, Kyoto University Hospital, Kyoto and [3]Pathology Project for Molecular Targets, The Cancer Institute, Japanese Foundation for Cancer Research, Tokyo, Japan

REFERENCES

1 Swerdlow SH, Campo E, Harris NL *et al.*, eds. *WHO Classification of Tumours of Haematopoietic and Lymphoid Tissues*. Geneva: WHO Press, 2008.
2 Morgan EA, Nascimento AF. Anaplastic lymphoma kinase-positive large B-cell lymphoma: An underrecognized aggressive lymphoma. *Adv Hematol* 2012; **2012**: 529572: 1–6.
3 Togashi Y, Soda M, Sakata S *et al.* KLC1-ALK: A novel fusion in lung cancer identified using a formalin-fixed paraffin-embedded tissue only. *PLoS One* 2012; **7**: e31323.
4 Van Roosbroeck K, Cools J, Dierickx D *et al.* ALK-positive large B-cell lymphomas with cryptic SEC31A-ALK and NPM1-ALK fusions. *Haematologica* 2010; **95**: 509–13.
5 Bedwell C, Rowe D, Moulton D, Jones G, Bown N, Bacon CM. Cytogenetically complex SEC31A-ALK fusions are recurrent in ALK-positive large B-cell lymphomas. *Haematologica* 2011; **96**: 343–46.
6 Wang WY, Gu L, Liu WP, Li GD, Liu HJ, Ma ZG. ALK-positive extramedullary plasmacytoma with expression of the CLTC-ALK fusion transcript. *Pathol Res Pract* 2011; **207**: 587–91.
7 Gascoyne RD, Lamant L, Martin-Subero JI *et al.* ALK-positive diffuse large B-cell lymphoma is associated with Clathrin-ALK rearrangements: Report of 6 cases. *Blood* 2003; **102**: 2568–73.
8 Delsol G, Lamant L, Mariamé B *et al.* A new subtype of large B-cell lymphoma expressing the ALK kinase and lacking the 2; 5 translocation. *Blood* 1997; **89**: 1483–90.
9 Takeuchi K, Soda M, Togashi Y *et al.* Identification of a novel fusion, SQSTM1-ALK, in ALK-positive large B-cell lymphoma. *Haematologica* 2011; **96**: 464–67.
10 Lee SE, Kang SY, Takeuchi K, Ko YH. Identification of RANBP2-ALK fusion in ALK positive diffuse large B-cell lymphoma. *Hematol Oncol* 2014. doi: 10.1002/hon.2125.